



NO 3 242 17

UFD 4-7

# RADIO CORPORATION OF AMERICA RCA LABORATORIES

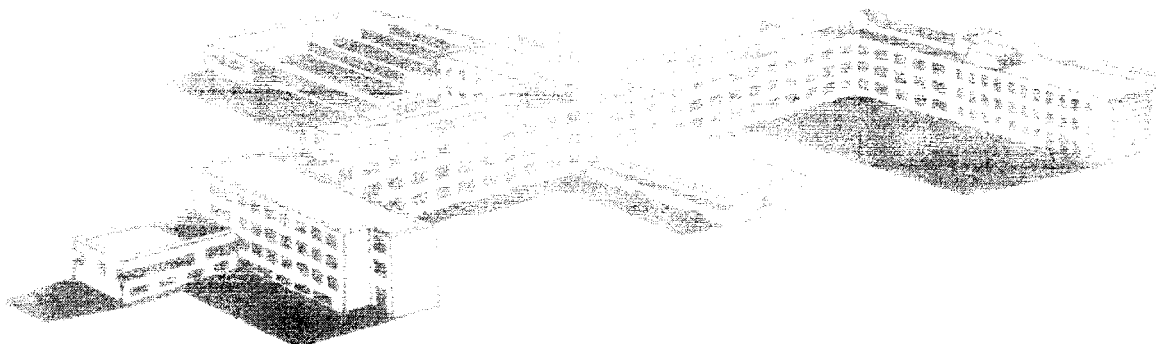
FIRST QUARTERLY REPORT  
FOR THE PERIOD  
OCTOBER 1, 1962 TO DECEMBER 31, 1962

## VAPOR-FILLED THERMIONIC CONVERTERS

CONTRACT NO. NAS 3-2531

JANUARY 23, 1963

NATIONAL AERONAUTICS AND SPACE ADMINISTRATION  
L-17 RESEARCH CENTER  
CLEVELAND, OHIO



DAVID SARNOFF RESEARCH CENTER  
PRINCETON, NEW JERSEY

FIRST QUARTERLY REPORT,  
~~FOR THE PERIOD~~  
OCTOBER 1, 1962 TO DECEMBER 31, 1962  
REPORT DATE: JANUARY 20, 1963

**VAPOR-FILLED THERMIONIC CONVERTERS**

*(NASA)*

CONTRACT NO. NAS 3-2531

NATIONAL AERONAUTICS AND SPACE ADMINISTRATION  
LEWIS RESEARCH CENTER  
CLEVELAND, OHIO

Prepared by: *checked*  
K. G. HERNQVIST, ~~Project Engineer~~  
J. R. FENDLEY *Gen. 20, 1963* *5 r/x*

Approved by: P. RAPPAPORT, Project Supervisor

*7364508*

RADIO CORPORATION OF AMERICA  
RCA LABORATORIES  
PRINCETON, NEW JERSEY

## ABSTRACT

*22249*

An analysis of the cesium vapor arc discharge is described. It is assumed that the discharge operates in the ball-of-fire mode, that cumulative ionization via the two resonance-excited states is the predominant ionization mechanism, and that trapping in the plasma of the resonance radiation results in a long effective lifetime of the states. A volt-ampere characteristic is derived for the cesium arc, and the results are applied to the thermionic energy converter. Good qualitative agreement is obtained between theory and experiment.

A tube for microwave studies of a cesium plasma is described. It is a duo-emitter diode having an ion emitter and an electron emitter facing each other. The incorporation of the tube in a microwave circuit is described.

A test station for the monitoring and control of the gas environment in an operating cesium diode is described. It is an all metal-ceramic system to which a mass spectrometer is attached for analysis of gases in the converter. Provisions are made for introducing different gases in addition to cesium.

*Author*

## TABLE OF CONTENTS

	<i>Page</i>
ABSTRACT .....	<i>ii</i>
I. ANALYSIS OF THE ARC MODE OF OPERATION OF THE CESIUM VAPOR THERMIONIC ENERGY CONVERTER.....	1
A. Arc Mode Thermionic Energy Converter .....	1
B. Theoretical Model for the Cesium Arc Discharge .....	3
C. Plasma Analysis .....	4
D. Application of Analysis to Thermionic Energy Converter .....	7
II. PLASMA STUDIES .....	11
III. TEST STATION .....	13
REFERENCES.....	16

## LIST OF ILLUSTRATIONS

<i>Figure</i>	<i>Page</i>
1 Idealized volt-ampere characteristic for thermionic energy converter .....	1
2 Experimental volt-ampere characteristic .....	2
3 Potential distribution for arc discharge of the ball-of-fire mode .....	3
4 Procedure to fit Eq. (18) to experimental V-I characteristic .....	8
5 Normalized volt-ampere characteristics; Eq. (18) with $I_p/I_s$ as a parameter .....	9
6 Fitting of theoretical volt-ampere characteristic to experimental data .....	9
7 Variation of electron temperature $T_e$ with current .....	10
8 Duo-emitter diode .....	11
9 Diode mounted in waveguide .....	11
10 Photograph showing duo-emitter mounted in waveguide .....	12
11 Gas analysis apparatus .....	14
12 Diagram of gas analysis apparatus .....	15

# I. ANALYSIS OF THE ARC MODE OF OPERATION OF THE CESIUM VAPOR THERMIONIC ENERGY CONVERTER

The ignited mode of operation of the thermionic energy converter can be classified as an externally heated hot cathode arc discharge. An analysis of this type of discharge had been partially completed before the initiation of this contract<sup>1</sup>. It is based on the following assumptions:

- (1) The arc is operating in the ball-of-fire mode<sup>2</sup>.
- (2) Ionization is predominantly proceeding via the two resonance-excited states of cesium (cumulative ionization).
- (3) Resonance trapping of the radiation results in a long effective lifetime of excited states.

This analysis has been carried on to include high current effects thus yielding a volt-ampere characteristic in good qualitative agreement with experimental data. A procedure for fitting the theoretical characteristic to the experimental characteristic has been developed which gives values for the contact difference of potential in agreement with values computed from electrode surface temperature and cesium vapor pressure data.

For completeness a brief summary of the foundations of the analysis is given here.

## A. ARC MODE THERMIONIC ENERGY CONVERTER

An idealized thermionic energy converter is a space-charge neutralized diode having a volt-ampere characteristic as shown in Fig. 1, which is a plot of the logarithm of the current vs.

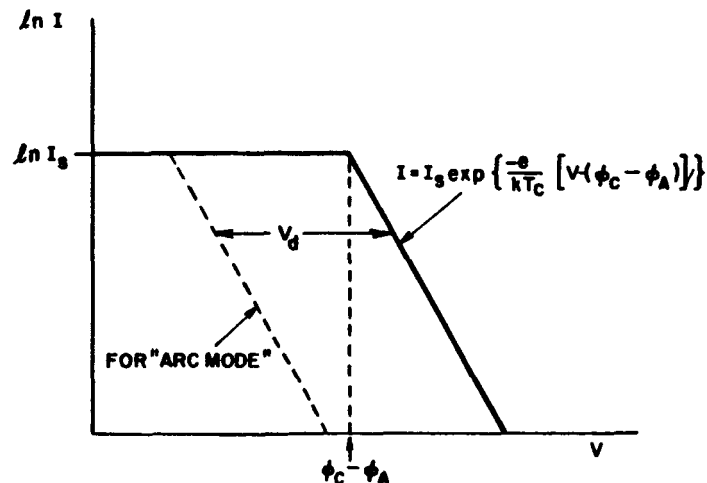


Fig. 1. Idealized volt-ampere characteristic for thermionic energy converter.

output voltage. The converter is a constant current generator (maximum current equal to the cathode saturated emission  $I_s$ ) up to an output voltage of  $\phi_c - \phi_A$ , where  $\phi_c$  = cathode work function and  $\phi_A$  = anode work function. For output voltages larger than  $\phi_c - \phi_A$ , the current falls off exponentially. In the arc mode of operation part of the potentially available output voltage is used internally in the diode to provide the necessary electrical power for plasma generation. If this internal arc drop  $V_d$  were independent of current (as is predicted by the analysis of Johnson<sup>2</sup>) the volt-ampere characteristic would be obtained by simply shifting the exponential line by an amount  $V_d$  as shown in Fig. 1. If  $V_d \geq \phi_c - \phi_A$  the characteristic would reduce to an exponential, the slope of which is determined by the cathode temperature.

A typical thermionic energy converter operating in the arc mode is a diode having a cathode-to-anode spacing of about a quarter of a millimeter and a cesium vapor pressure of the order of 1 millimeter of mercury. The volt-ampere characteristic of such a device<sup>3</sup> is shown in Fig. 2. In this converter the cathode temperature  $T_c$  was 1200°C, the anode temperature was 550°C, and the cesium reservoir temperature was 310°C. Both cathode and anode were cesium-covered molybdenum yielding estimated work functions of  $\phi_c = 2.2$  volts and  $\phi_A = 1.7$  volts corresponding to a contact difference of potential of 0.5 volts. The cathode area was 2.48 cm<sup>2</sup>. In Fig. 2 is also

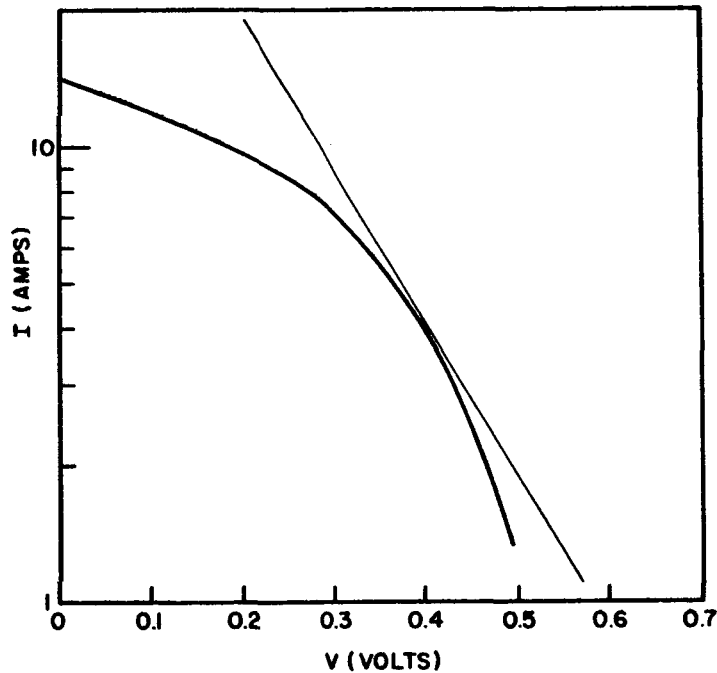


Fig. 2. Experimental volt-ampere characteristic.

plotted the exponential line of slope  $\frac{e}{kT_c}$  ( $e$  = electronic charge and  $k$  = Boltzman constant) arbitrarily positioned to the right of the experimental volt-ampere characteristic. The deviation from the exponential behavior is evident both at high and low currents. The behavior at low current is particularly noteworthy. Characteristics have been observed where the deviation at lower currents is so pronounced as to lead to a change of sign in the slope of the volt-ampere characteristic.

## B. THEORETICAL MODEL FOR THE CESIUM ARC DISCHARGE

The ball-of-fire mode of hot-cathode arcs is characterized<sup>1</sup> by a potential distribution between the cathode and the anode as shown in Fig. 3. A small retarding-field region near the cathode is followed by a rise in potential in a space-charge sheath joined to the main plasma, in

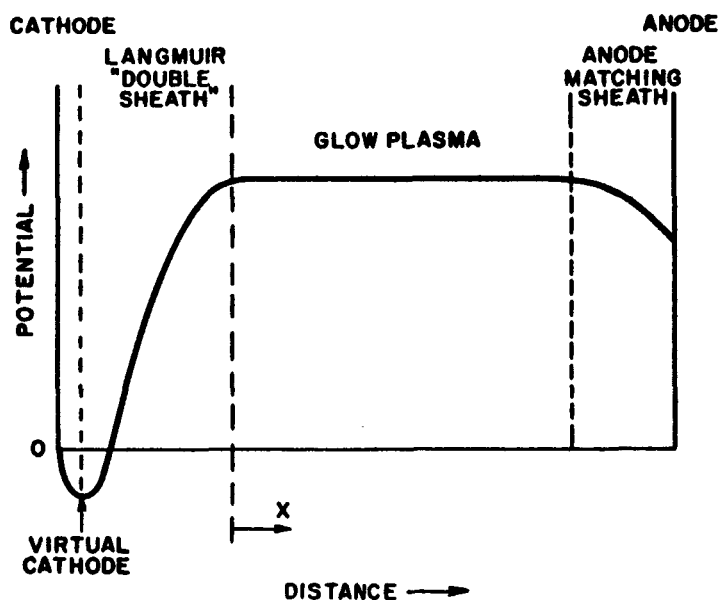


Fig. 3. Potential distribution for arc discharge of the ball-of-fire mode.

which impact ionization occurs. This plasma is joined to the anode by another retarding-field region for the electrons. Electrons accelerated into the plasma region are thermalized and the plasma is characterized by a relatively high electron plasma temperature  $T_e$ . Probe measurements<sup>4</sup> and visual inspection<sup>1</sup> of the light emitted from the interelectrode space of a cesium vapor converter qualitatively corroborates this model.

Energy balance for the discharge requires that the power input equals power sinks. Thus

$$\underbrace{V_d I}_{\text{Electrical Input}} + \underbrace{\frac{2kT_c}{e} I}_{\text{Power Taken From Cathode By Emitted Electrons}} = \underbrace{\frac{2kT_e}{e} I}_{\text{Power Delivered To Anode By Hot Plasma Electrons}} + \underbrace{V_i I_p}_{\text{Ionization}} + \underbrace{P_{rad}}_{\text{Light Radiation}} + \underbrace{P_{rec}}_{\text{Particle Recombination}} \quad (1)$$

where  $I$  = electron current,  $I_p$  = ion current,  $T_c$  = cathode temperature, and  $V_i$  = ionization potential. The first term of the right hand side is dominating<sup>4</sup>; thus, to a first approximation the maximum output voltage becomes

$$V = \phi_{c_{eff}} - \phi_A - \frac{2k}{e} (T_e - T_c) \quad (2)$$

where

$$\phi_{c_{eff}} = \phi_c \quad \text{for} \quad I \geq I_s$$

$$\phi_{c_{eff}} = \frac{kT_c}{e} \ln \frac{ABT_c^2}{I} \quad \text{for} \quad I < I_s$$

Here  $A$  = cathode area and  $B$  = electron emission constant. It is evident from Eq. (2) and Fig. 2 that  $T_e$  is not current-independent as predicted by the original ball-of-fire analysis. Comparison of Eq. (2) with the experimental  $V$ - $I$  characteristic of Fig. 2 suggests that the electron temperature for small currents decreases with current and reaches a minimum after which it again increases at higher currents.

In the present analysis it will be postulated that cumulative ionization is a dominant process. Here ions are formed by impact ionization of excited atoms, mainly of the two resonance states  $2P_1$  and  $2P_2$ . These states, which are located, respectively, 1.38 and 1.45 volts above the ground state, have natural lifetimes of the order of  $10^{-8}$  sec. However, experiments indicate<sup>1</sup> that due to resonance trapping of the radiation the effective lifetime may be several orders of magnitude higher. No attempts will be made in this analysis to evaluate the photon diffusion problem. Rather, an approximate average effective lifetime will be assigned to each excited atom.

The plasma electron temperature is determined by equating the rate of loss of ions from the plasma and the rate of production of ions.

### C. PLASMA ANALYSIS

Analysis of the electron and ion diffusion problem for the plasma yields the ion loss rate per unit volume



$$\frac{dN}{dt} = N \left( \frac{2.18}{d} \sqrt{\frac{kT_e}{3m_p}} + \sigma N \right) \quad (3)$$

and the electron current density

$$j = eN \sqrt{\frac{kT_e}{3m_e}} \quad (4)$$

where

$N$  = plasma density,

$d$  = cathode-to-anode distance,

$m_p$  and  $m_e$  = the ion and electron mass, respectively,

$\sigma$  = volume recombination coefficient.

For the case of stepwise ionization it is convenient to write for the number of excited atoms  $\mathcal{H}_x$  formed per meter path per electron

$$\mathcal{H}_x = p a_x (V - V_x) \quad (5)$$

where  $p$  is the gas pressure in mm of Hg,  $V_x$  is the excitation potential, and  $a$  is the differential excitation coefficient. In terms of actual neutral gas density  $N_n$  expressed in number of neutral and unexcited atoms per cubic meter, Eq. (5) becomes

$$\mathcal{H}_x = \frac{N_n}{n} a_x (V - V_x) \quad (6)$$

where

$$n = 3.56 \times 10^{22} \frac{273}{T_g}$$

$T_g$  = gas temperature in °K.

For a plasma having a Maxwellian velocity distribution for electrons of density  $N$  electrons per  $m^3$ , the number of excited atoms generated per second per electron becomes<sup>1</sup>

$$\mathcal{H}_x = \sqrt{\frac{8kT_e}{\pi m_e}} a_x \frac{N_n}{n} \left( V_x + \frac{2kT_e}{e} \right) e^{-eV_x/kT_e} \quad (7)$$

Similarly the number of ions generated (from excited atoms of state  $x$ ) per second per electron becomes

$$\mathcal{Q}_{xi} = \sqrt{\frac{8kT_e}{\pi m_e}} a_{xi} \frac{N_x}{n} \left( V_{xi} + \frac{2kT_e}{e} \right) e^{-eV_{xi}/kT_e} \quad (8)$$

where

$a_{xi}$  = differential ionization coefficient (referred to ionization of excited atoms)

$V_{xi} = V_i - V_x$

$N_x$  = density of excited states in  $m^{-3}$ .

$N_x$  is determined by equating generation rate of excited states to the sum of the different loss rates,

$$N\mathcal{Q}_x = \frac{N_x}{\tau} + N\mathcal{Q}_{xi} + N\mathcal{Q}_{xo} \quad (9)$$

where  $\tau$  is the effective average lifetime of excited states in absence of quenching collisions, and  $\mathcal{Q}_{xo}$  is the quenching rate due to collisions not leading to ionization. Due to the Maxwellian velocity distribution of electrons, most quenching collisions are of this second class. It is convenient to express  $\mathcal{Q}_{xo}$  in terms of the frequency  $f_o$  of quenching collisions between electrons and neutrals at a cesium pressure of 1 mm of Hg; thus,

$$\mathcal{Q}_{xo} = f_o \frac{N_x}{n} \quad (10)$$

At higher degrees of ionization and excitation the density of neutral cesium atoms in the ground state may be appreciably lower than the actual gas density, or

$$N_n = N_g - N_x - N \quad (11)$$

where  $N_g = np$ .

Equations (5) through (11) may now be re-arranged to yield

$$\mathcal{Q}_{xi} = N \frac{\frac{8kT_e}{\pi m_e} a_x a_{xi} \left( V_x + \frac{2kT_e}{e} \right) \left( V_{xi} + \frac{2kT_e}{e} \right) e^{-eV_i/kT_e} \left( \frac{N_g - N}{n} \right)}{\frac{n}{\tau} + N \sqrt{\frac{8kT_e}{\pi m_e}} \left[ a_x \left( V_x + \frac{2kT_e}{e} \right) e^{-eV_x/kT_e} + a_{xi} \left( V_{xi} + \frac{2kT_e}{e} \right) e^{-eV_{xi}/kT_e} \right] + N f_o} \quad (12)$$

Equation (12) determines the ion generation rate supported by a certain electron temperature  $T_e$ . Equations (3) and (4) determine the ion generation called for at a certain electron current density  $j = I/A$ , where  $A$  = cathode area. Combining Eqs. (3), (4), and (12) yields the relation between current and electron temperature

$$T_e = \frac{eV_i}{k} \ln^{-1} \left\{ \frac{1}{I_r} \left[ 1 - \frac{N_0}{N_g} - \frac{2\gamma_{xi}}{\sqrt{\frac{8kT_e}{\pi m_e}}} \left( \frac{e^{eV_{xi}/kT_e}}{v_{xi} + \frac{2kT_e}{e}} + \frac{e^{eV_x/kT_e}}{v_x + \frac{2kT_e}{e}} \right) \right] \right\} \quad (13)$$

where

$$I_r = 0.285 \frac{Ae n \sqrt{m_e/m_p}}{d p \sum_a \tau_a a_{x_a} a_{x_{ai}} \left( v_{x_a} + \frac{2kT_e}{e} \right) \left( v_{x_{ai}} + \frac{2kT_e}{e} \right)} \quad (14)$$

$$\gamma = \sqrt{\frac{3m_e}{kT_e}} \frac{\tau f_0}{n A_e} \quad (15)$$

$$\mathcal{H} = 1.38 \frac{\sigma d \sqrt{m_e m_p}}{e A T_e} \quad (16)$$

In Eq. (14) the sum is to be taken over the  $a$  excited states considered.

#### D. APPLICATION OF ANALYSIS TO THERMIONIC ENERGY CONVERTER

Introducing the saturated electron emission current from the cathode, Eqs. (2) and (13) become

$$V \cong \phi_c - \phi_A + \frac{2kT_c}{e} + \frac{kT_c}{e} \ln \frac{I_s}{I} - \frac{2V_i}{\ln \frac{I_s}{I_r} - \ln \frac{I_s}{I} - \ln(1+\gamma I) - \ln(1+\mathcal{H} I)} \quad (17)$$

for low degrees of ionization ( $N_N \approx N_g$ ). Using normalized voltage variables, Eq. (17) can be rewritten as

$$\eta = \eta_\psi + \ln \frac{I_s}{I} - \frac{2\eta_i}{\ln \frac{I_s}{I_r} - \ln \frac{I_s}{I} - \ln(1+\gamma I) - \ln(1+\mathcal{H} I)} \quad (18)$$

where

$$\eta = \frac{eV}{kT_c}, \quad \eta_\psi = \frac{e}{kT_c} \left( \phi_c - \phi_A + \frac{2kT_c}{e} \right), \text{ and } \eta_i = \frac{eV_i}{kT_c}.$$

The quantity  $(\eta - \eta_{\psi})$  has been plotted as a function of  $I/I_s$ , as in Fig. 4 with  $I_r/I_s$  a parameter and assuming  $\gamma = \mathcal{H} = 0$ ,  $V_i = 3.88$  volts, and  $T_c = 1200^\circ\text{C}$ .

The procedure for actual fitting of Eq. (18) to experimental data is shown schematically in Fig. 4. The experimental volt-ampere curve is first plotted in the form  $\ln I_s/I$  versus  $\eta$ , where  $I_s$  is arbitrarily chosen as the short-circuit current. Of the curves shown in Fig. 5 one is chosen

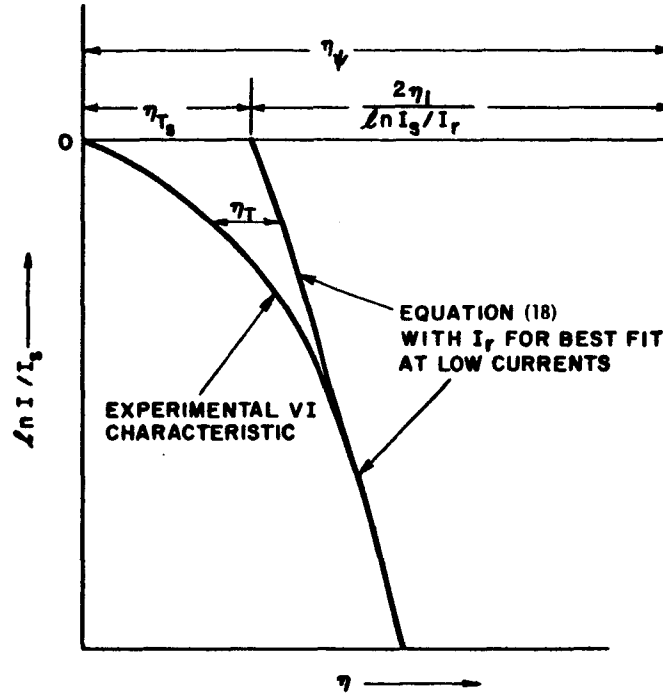


Fig. 4. Procedure to fit Eq. (18) to experimental VI characteristic.

that gives the best fit for small currents where the approximation  $\gamma = \mathcal{H} = 0$  is valid. This procedure yields  $I_r$ . The deviation between the experimental curve and Eq. (18) for  $\gamma = \mathcal{H} = 0$  is called  $\eta_T$ . Thus, the actual electron temperature becomes

$$T_e = T_c \left( \frac{\eta_i}{\ln \frac{I_s}{I_r} - \ln \frac{I_s}{I}} + \frac{1}{2} \eta_T \right) \quad (19)$$

and the contact difference of potential becomes

$$\phi_c - \phi_A = \frac{kT_c}{e} \left[ \frac{2\eta_i}{\ln \frac{I_s}{I_r}} + \eta_{Ts} - 2 \right] \quad (20)$$

where  $\eta_{Ts}$  is defined in Fig. 4.

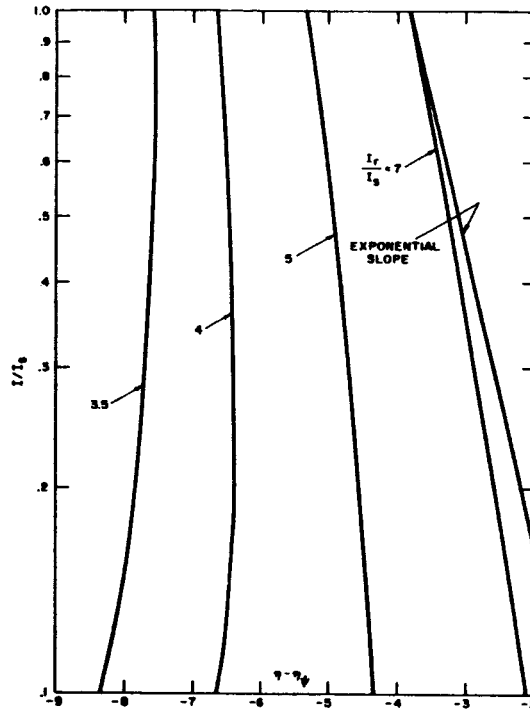


Fig. 5. Normalized volt-ampere characteristics; Eq. (18) with  $I_r/I_s$  as a parameter.

Figure 6 shows the fitting of the experimental curve of Fig. 2 to Eq. (18) with  $\gamma = \mathcal{H} = 0$  and  $I_s/I_r = 10^7$ . The variation of electron temperature with current as obtained from Eq. (19) is shown in Fig. 7. Note the characteristically low electron temperatures, which are comparable to those obtained by probe measurements<sup>4</sup>. Using Eq. (20) a value for the contact difference of potential of 0.5 volt is obtained, which is in agreement with the value estimated from electrode temperatures and cesium pressure.

An estimate of the order of magnitude of the differential excitation coefficients  $a_x$  and  $a_{xi}$  can be had if the value of  $I_s/I_r = 10^7$  is used in Eq. (13). Considering the two resonance states of cesium ( $V_x = 1.38$ ,  $V_{xi} = 2.52$  and  $V_x = 1.45$ ,  $V_{xi} = 2.45$ ), assuming  $a_x$ ,  $a_{xi}$  and  $\tau$  to be equal for the two states, and using the experimental values for  $d = 1/4$  mm,  $p = 2.5$  mm of mercury,  $j_s = 5.7$  A/cm<sup>2</sup>, and  $\tau = 10^{-5}$  sec (Ref. 1), Eq. (13) yields  $a_x a_{xi} \approx (60000)^2$ . These values for the coefficients  $a_x$  and  $a_{xi}$  are quite reasonable, being about one order of magnitude higher than measured values<sup>5</sup> for the ionization coefficient  $a_i \approx 2000$  (meter  $\times$  volt  $\times$  mm of Hg)<sup>-1</sup>.

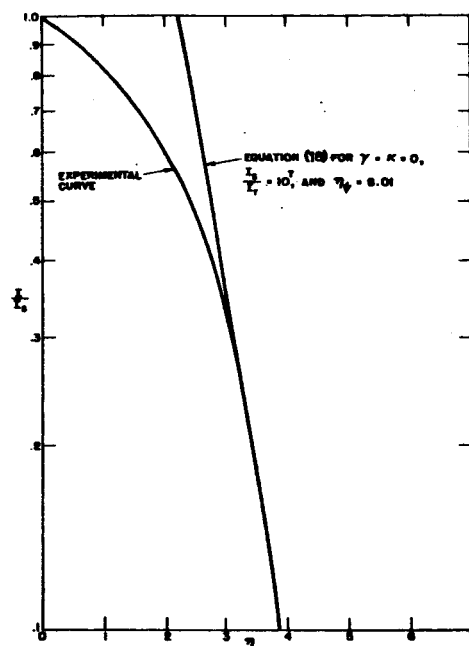


Fig. 6. Fitting of theoretical volt-ampere characteristic to experimental data.

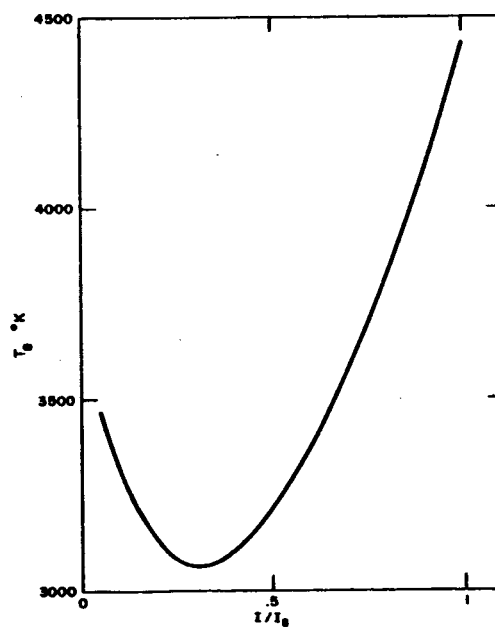


Fig. 7. Variation of electron temperature  $T_e$  with current.

## II. PLASMA STUDIES

For microwave studies of a cesium plasma a duo-emitter diode was built which can be made a part of a microwave transmission system. The duo-emitter diode has a 1/4-in. diameter flat L-cathode facing a hafnium ion emitter of the same diameter. The emitters are spaced 1/2 in. apart. The diode is installed in a rectangular waveguide so that the plasma acts as a shorting stub across the waveguide. An RG-(50)/U waveguide was chosen allowing plasma diagnostics in the frequency range 5.8 to 8.2 kMc. The tube (shown in Fig. 8) is of all metal-ceramic construction. Figures 9 and 10 show how the tube is installed in the waveguide. An electromagnet provides an axial magnetic field for confinement of the plasma into a well defined cylinder. It is planned to perform measurements on this diode operated both in the plasma synthesis mode and in the arc discharge mode.

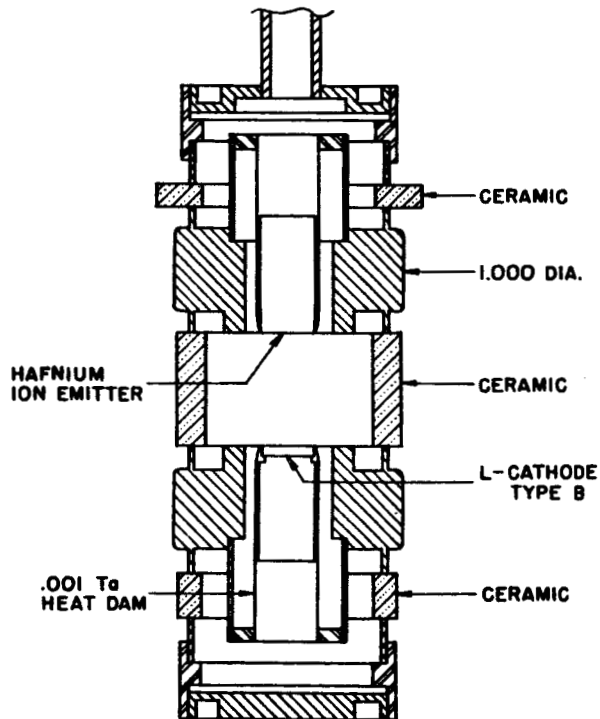


Fig. 8. Duo-emitter diode.

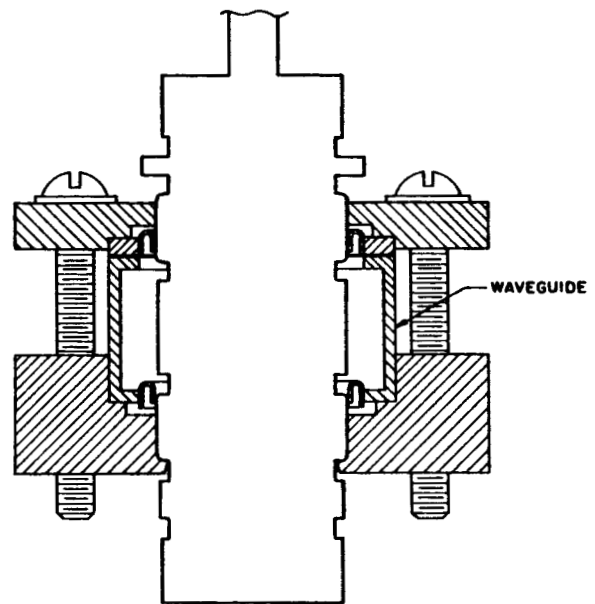


Fig. 9. Diode mounted in waveguide.

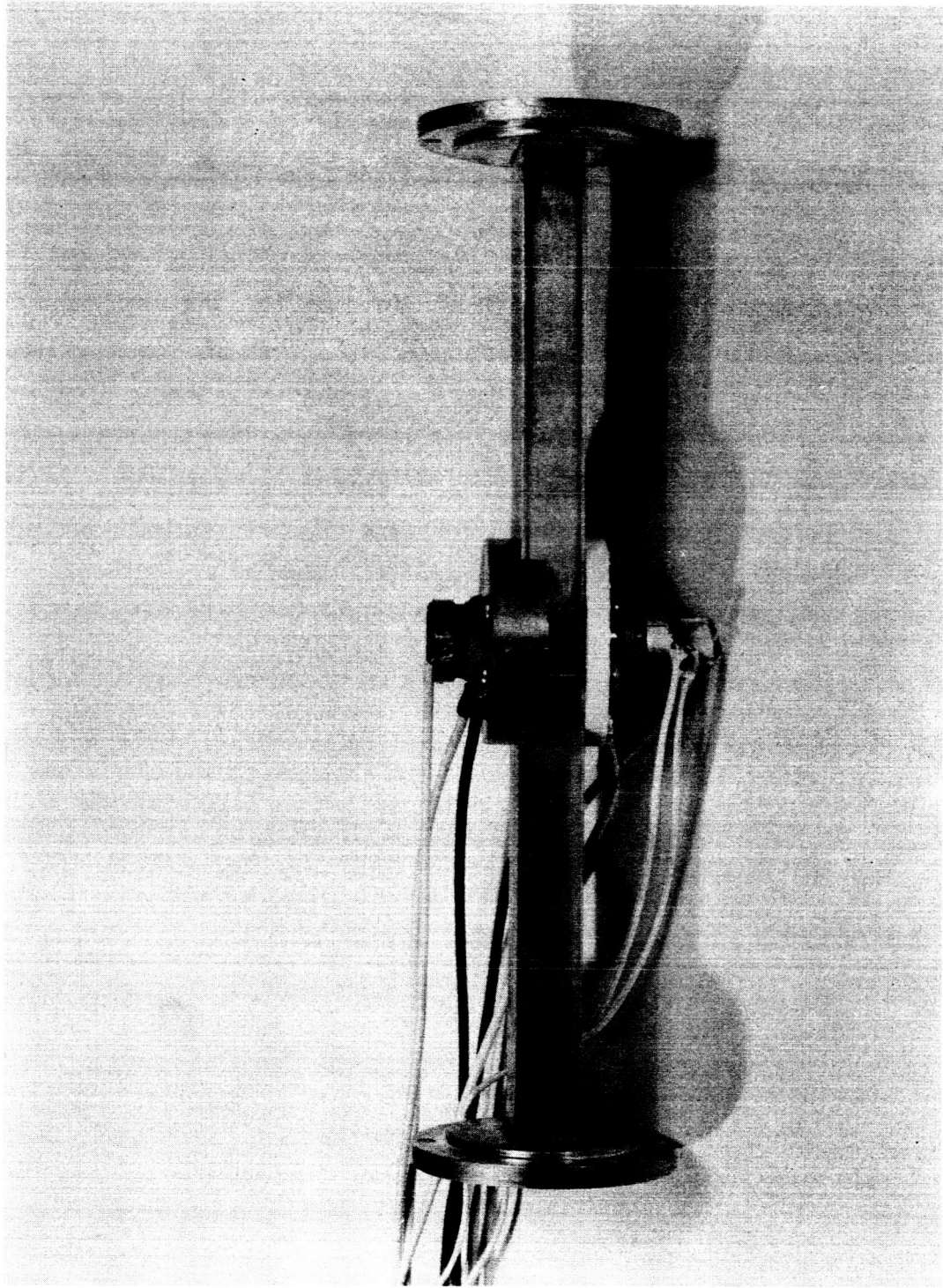


Fig. 10. Photograph showing duo-emitter diode mounted in waveguide.



### III. TEST STATION

Apparatus is being constructed for monitoring and controlling the gas pressure in an operating cesium diode. A photograph of this apparatus is shown in Fig. 11 and a drawing is shown in Fig. 12.

The photograph shows a thermionic converter diode with sapphire window attached to the test station. The converter was built by the RCA Electron Tube Division. Below the converter is a spare cesium capsule. To the left of the tube is a stainless steel tee with a cesium reservoir appended to the bottom. Connected to the top part of this tee is a copper distillation elbow.

The temperature along this elbow will range from the cesium boiler temperature ( $\sim 300^{\circ}\text{C}$ ) to a temperature slightly above the melting point of cesium ( $\sim 40^{\circ}\text{C}$ ). Most of the cesium vapor which rises in the distillation elbow will be condensed and drip back into the boiler. The cesium which emerges from the top of the elbow will be frozen in the stainless steel U-tube cold trap.

An 8 liter/second getter-ion pump allows removal of non-condensable gas. Also connected to the high-vacuum manifold is an AEI model MS-10 mass spectrometer tube and a variable leak. The leak is backed in the open position, and through it are pumped gases which come from the heater chamber of the converter tube. An insulating spool section allows heater voltage to be applied to the tube.

The apparatus as shown has been baked for 15 hours at  $275^{\circ}\text{C}$ . Bakeout up to  $400^{\circ}\text{C}$  is permissible and will be done.

When the heater chamber is thoroughly outgassed, the 1/4-in. copper tubing connecting this chamber to the pump will be pinched off. Then the variable leak may be used for the introduction of whatever gas is desired.

Introduction of  $\text{H}_2$ ,  $\text{CO}$  and  $\text{O}_2$  is planned. Effect of the various gases on the electrical characteristics of the converter will be studied. Also, the gases evolved inside the tube during operation will be analyzed by the mass spectrometer.

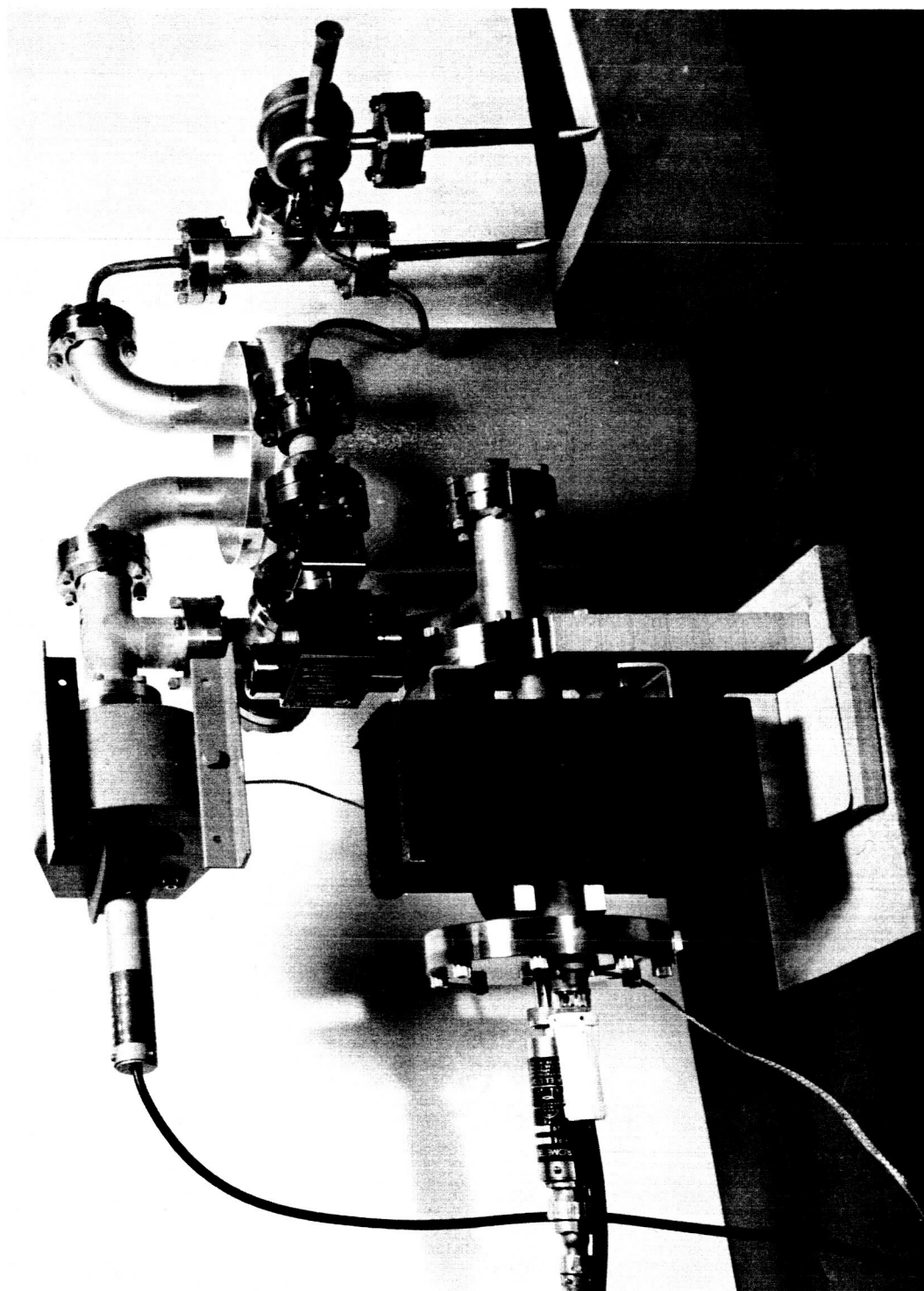


Fig. 11. Gas analysis apparatus.

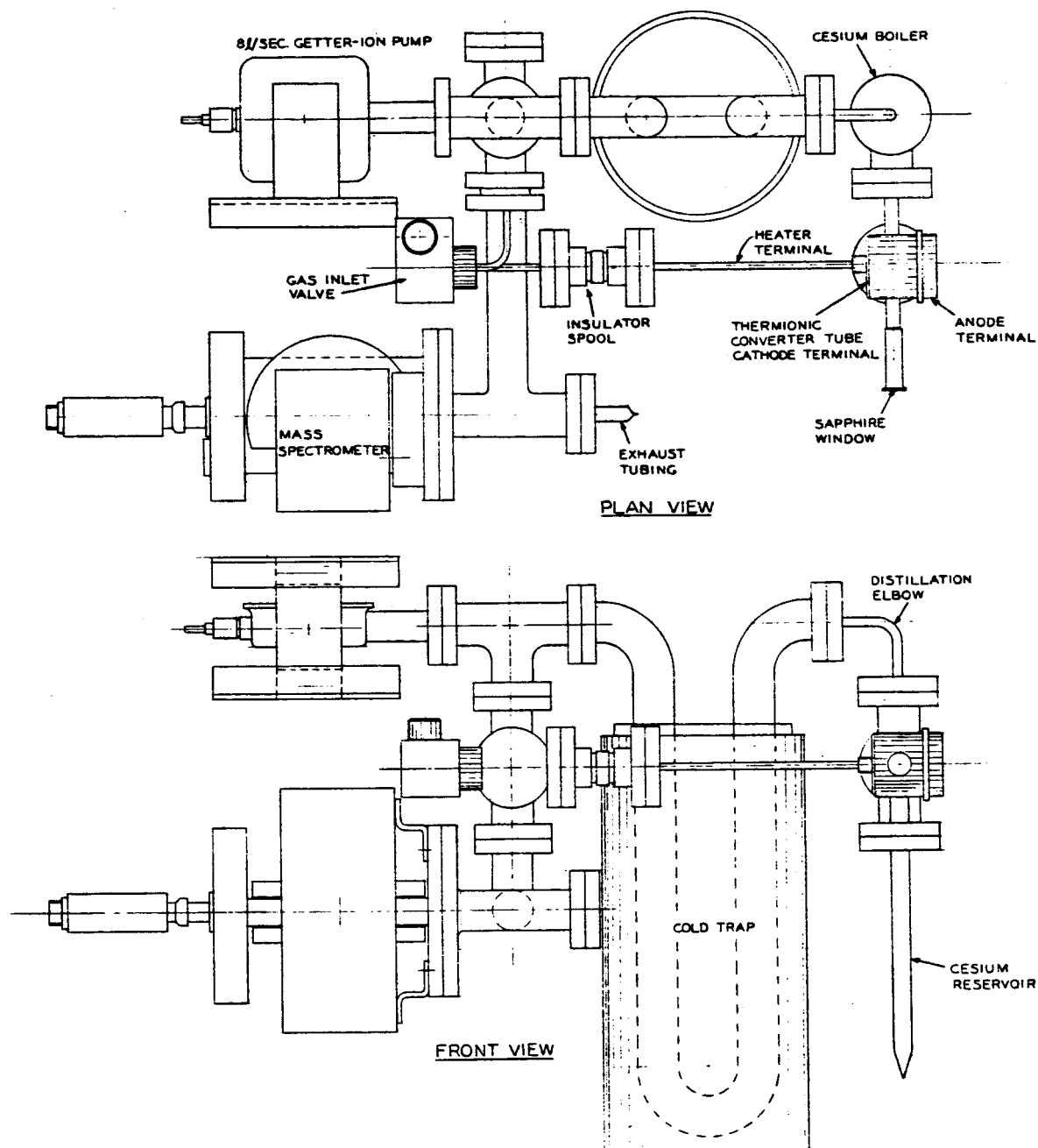


Fig. 12. Diagram of gas analysis apparatus.

## REFERENCES

1. "Development of a Low-Temperature, Vapor-Filled Thermionic Converter for Nuclear Applications," Summary Technical Report, August 1962, Contract NObsr 84823, pages 67-80.
2. E. O. Johnson, *RCA Review* **16**, 498 (1955).
3. "The Development of a Low-Temperature, Vapor-Filled Thermionic Converter," Tech. Documentary Report ASD-TDR-62-324, April 1962, Contract No. AF33(616)-7903.
4. N. D. Morgulis and Yu. P. Korchevoi, *Radio Engineering and Electronic Physics*, 1859, Dec. 1961.
5. W. B. Nottingham, "Ionization of Cesium at Surfaces," *MIT Tech. Rep.* **405**, August 17, 1962.